# Precision Shaping, Assembly and Metrology of Foil Optics for X-ray Reflection Gratings

Craig R. Forest[a], Mark L. Schattenburg[a], Carl G. Chen[a], Ralf K. Heilmann[a], Paul T. Konkola[a], JoHanna Przbylowski[a], Yanxia Sun[a], Jenny You[a], Steven M. Kahn[b], and Don Golini[c]

[a]Massachusetts Inst. of Technology, Center for Space Research, Cambridge, MA 02139, USA
[b]Columbia University, Department of Physics, New York, NY 10027
[c]QED Technologies, Inc., Rochester, NY 14607

## ABSTRACT

The proposed Reflection Grating Spectrometer (RGS) on the *Constellation–X* mission is designed to provide high-resolution x-ray spectroscopy of astrophysical sources. Two types of reflection grating geometries have been proposed for the RGS. In-plane gratings have relatively low-density rulings ($\sim$500 lines/mm) with lines perpendicular to the plane of incidence, thus dispersing x-rays into the plane. This geometry is similar to the reflection grating spectrometer flown on the *X-ray Multi-Mirror* (XMM) mission. Off-plane, or conical, gratings require much higher density rulings (>5000 lines/mm) with lines parallel to the plane of incidence, thus dispersing x-rays perpendicular to the plane. Both types present unique challenges and advantages and are under intensive development. In both cases, however, grating flatness and assembly tolerances are driven by the mission's high spectral resolution goals and the relatively poor resolution of the Wolter foil optics of the Spectroscopy X-ray Telescope (SXT) that is used in conjunction with the RGS. In general, to achieve high spectral resolution, both geometries require lightweight grating substrates with arcsecond flatness and assembly tolerances. This implies sub-micron accuracy and precision which go well beyond that achieved with previous foil optic systems. Here we present a progress report of technology development for the precision shaping, assembly and metrology of the thin, flat grating substrates.

**Keywords:** x-ray telescopes, reflection gratings, Constellation-X, mirror alignment, precision assembly, MEMS, Shack-Hartmann, metrology, wavefront sensing, magneto-rheologic finishing, MRF

## 1. INTRODUCTION

The Reflection Grating Spectrometer (RGS) on *Constellation–X* requires the accurate shaping, patterning and assembly of thousands of thin, flat grating substrates. Depending on the particular grating geometry, grating substrates are generally rectangular with dimensions on the order of 100–200 mm and thickness ranging from 0.4–2 mm. A variety of substrate materials have been proposed including glass, silicon and silicon carbide.

Grating patterning on thin substrates poses a number of interesting technical problems whose detailed treatment is beyond the scope of this paper. In particular, traditional patterning schemes such as replication have required thick, stiff substrates that consume a large fraction of the total mass budget. Several advanced patterning schemes that are more amenable to thin substrates are under development in our laboratory, each of which places particular constraints on the substrate material and stiffness. However, all proposed schemes require the accurate shaping, assembly, and metrology of thin substrates.

To meet mission spectral resolution goals, substrates need to be accurately shaped and assembled such that the grating surfaces deviate from the desired flat surfaces by no more than a few arcseconds. This requires

Further author information: (Send correspondence to C.R.F.)
C.R.F.: E-mail: cforest@mit.edu, Telephone: 1 617 253 5877
M.L.S.: E-mail: marks@space.mit.edu, Telephone: 1 617 253 3180, Address: Space Nanotechnology Laboratory, Center for Space Research, Massachusetts Institute of Technology, 70 Vassar St., 37-487, Cambridge, MA 02139



X-Ray and Gamma-Ray Telescopes and Instruments for Astronomy, Joachim E. Trümper, Harvey D. Tananbaum, Editors, Proceedings of SPIE Vol. 4851 (2003)

substrates to be shaped flat and assembled to tolerances of a small fraction of a micron. While a variety of promising thin substrate shaping technologies are under development in our laboratory, we limit our discussion here to just one: magneto-rheologic finishing (MRF), which is presented in Sect. 2.

Also under development in our laboratory is a method for assembling nested, segmented foil optics with sub-micron accuracy and repeatability using lithographically manufactured silicon alignment structures, called microcombs.[1] A system of assembly tooling incorporating the silicon microstructures, called an assembly truss, is used to position the foils that are then bonded to a spaceflight module. The advantage of this procedure is that the flight module has relaxed tolerance requirements while the precision assembly tooling can be reused.

Previous work demonstrated that microcombs can provide accurate and repeatable reference surfaces for the optic foils.[2] Current research has developed a second-generation device that makes progress towards actual flight module assembly. Key features include flexure bearings for frictionless motion of the microcombs, kinematic couplings to ensure repeatable alignment of successive flight modules and flight module integration. Thin substrates require special considerations for subtle effects, such as the distorting effects of gravity sag, contact friction and pinching during assembly, and thermal expansion mismatch, that can often be safely ignored for thicker, stiffer substrates. The new tooling is designed to study and mitigate these effects. Details of our second-generation assembly truss design and performance are presented in Sect. 3.

Progress in our laboratory towards the *Constellation–X* RGS goals has been slowed by a lack of accurate surface and assembly metrology. In addition to sub-micron assembly tolerances, individual foils must be manufactured with figure errors that are a small fraction of a micron. Accurate metrology is essential to confirm the efficacy of substrate flattening processes and to provide active metrological feedback during assembly procedures. In Sect. 4 we report on the performance of a novel deep-UV Shack-Hartmann surface metrology tool developed for this purpose. The use of deep-UV wavelengths is particularly useful for studying transparent substrates such as glass which are virtually opaque to wavelengths below 260 nm.

## 2. FOIL OPTIC SHAPING TECHNOLOGY

The shaping of thin optics poses one of the more difficult and interesting challenges of reflection grating development. During the shaping of substrates using traditional optical figuring techniques, opticians generally require that substrates be no thinner than 15% of their diameter in order to prevent loss of accuracy due to distortion during polishing. However, foil optic substrates can be thinner than 1% of the substrate dimensions. The foil's lack of stiffness obviates traditional flattening methods such as double-sided polishing which simply result in warped parts that are very uniform in thickness.

We are continuing to investigate several promising methods for shaping thin sheets, including block lapping and thermal shaping.[3] More recently we have investigated a method called magneto-rheologic finishing (MRF). The principle is illustrated in Fig. 1. During MRF figuring, a workpiece is first measured using a surface metrology tool such as an interferometer to characterize its deviation from the desired shape. It is then placed in the polishing tool and brought into proximity with a spinning sphere. A magneto-rheologic polishing fluid is then entrained onto the surface of the sphere that carries it to the region of minimum gap between the workpiece and sphere. A magnetic field that is focused in this region stiffens the fluid and causes abrasive removal of the surface. By translating the workpiece on an X-Y table and controlling the dwell time, a programmed amount of surface can be removed as determined by the surface metrology. Unlike traditional polishing, MRF polishing applies no pressure normal to the surface, resulting in a deterministic removal function immune to substrate holding forces.

Figure 2 shows surface topography maps of a 100 mm diameter, 450 $\mu$m thick silicon wafer that was measured before and after MRF processing. The surface figure has been reduced from 6.55 $\mu$m to 0.81 $\mu$m, peak-to-valley (P-V). To our knowledge, these are the flattest wafers ever produced. This wafer's initial non-flatness is typical. Surface roughness has remained the same or slightly improved, which is acceptable. Further progress beyond this point has been hampered by the poor quality of our surface metrology. Our new Shack-Hartmann system (see Sect. 4) should help us to reduce the metrology error and enable much flatter substrates.

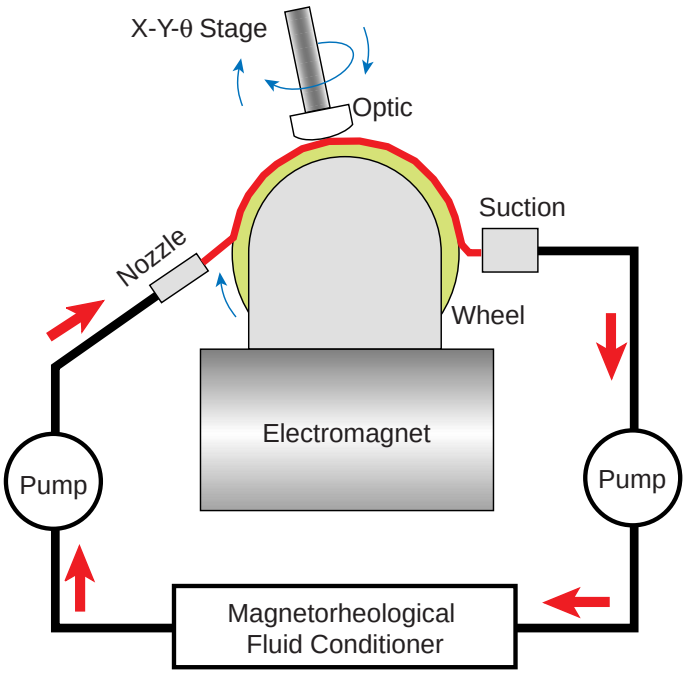


**Figure 1.** Principle of Magneto-Rheologic Fluid Polishing.

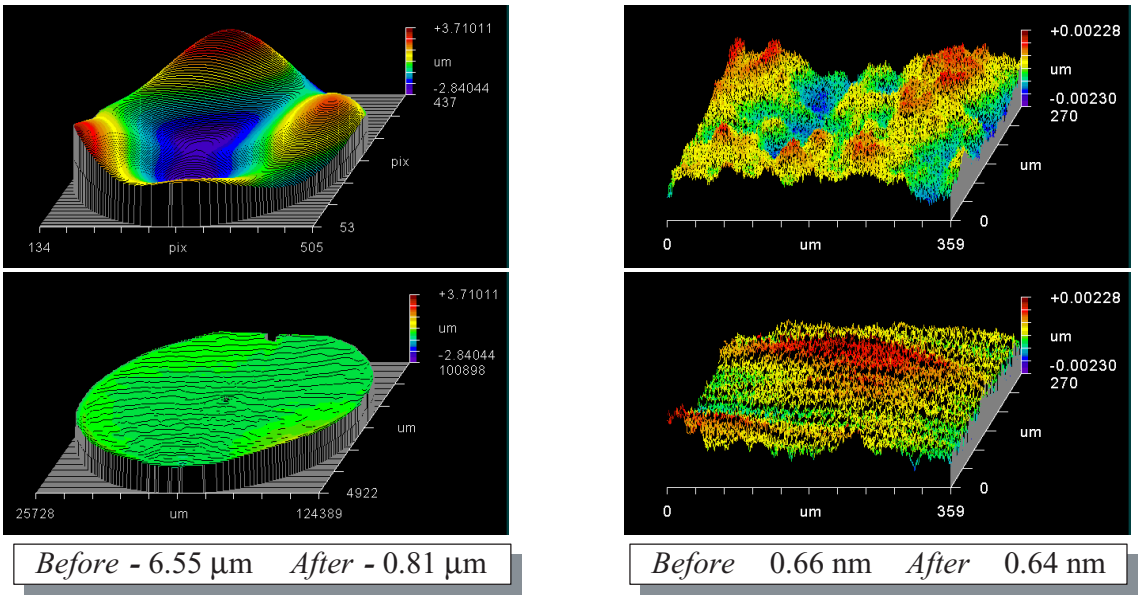


**Figure 2.** MRF polishing effect on silicon wafer surface figure (*left*) and surface roughness (*right*).

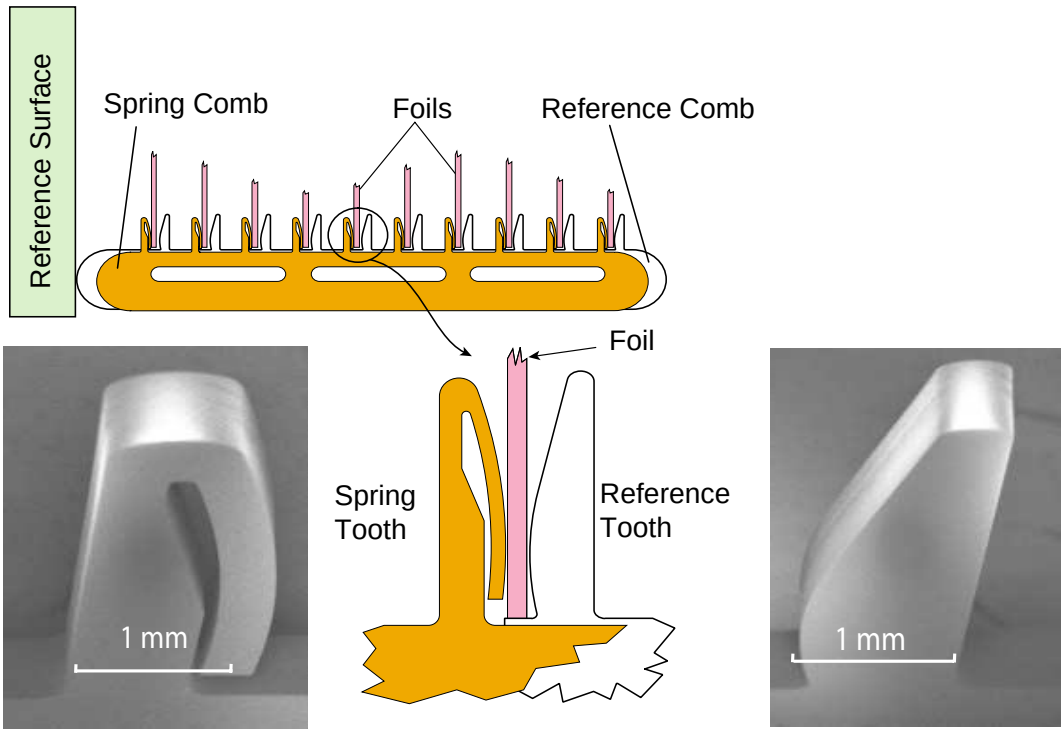


**Figure 3.** Silicon microcombs establish an accurate and repeatable metrology frame. Scanning electron microscope images of the combs show their respective sizes.

## 3. PRECISION FOIL ASSEMBLY TRUSS

A foil optic assembly tool has been developed to overcome the challenges of aligning the *Constellation–X* reflection gratings. This device has been designed to prove that tens of foil optics can be assembled accurately and repeatably to sub-micron tolerances. Accuracy of foil assembly will be essential to achieving spectral resolution goals within a single spaceflight module. Repeatability is required since the assembly tooling must be reused to align the foils in numerous spaceflight modules. The current work has demonstrated synchronous sub-micron precision alignment of a set of foils.

### 3.1. Design

The assembly truss design utilizes lithographically manufactured microcombs to provide accurate and repeatable reference surfaces for optic foil alignment. This fundamental aspect of the device is illustrated in Fig. 3. Two types of microcombs, spring and reference, are used in conjunction to position the foils. First, the reference comb is driven into contact with a reference surface, thereby accurately locating each of its teeth. The spring comb is subsequently actuated to force the foils against these reference teeth.

The entire assembly tool is shown in Fig. 4. To constrain the optic foils, this device contains two microcomb sets on the base and one microcomb set on the cover. These microcomb sets are supported by monolithic flexure bearings as shown in Fig. 5. There is a flexure bearing for each microcomb and these provide hysteresis-free, friction-free bearings for reference combs to make contact with the reference flat and for the spring combs to impart forces to the foil. The flexures have been manufactured from stress relieved aluminum 6061-T651 to prevent warping due to the release of internal stresses during manufacture. The four bar linkage design of the flexure bearings allows parallel motion between the top and bottom members. In fact, a parasitic pitch error in this motion is virtually eliminated with proper selection of the position of the driving point.[4] The flexures are actuated at half of their height by differential screw micrometers (Mitutoyo, model 110-102) which

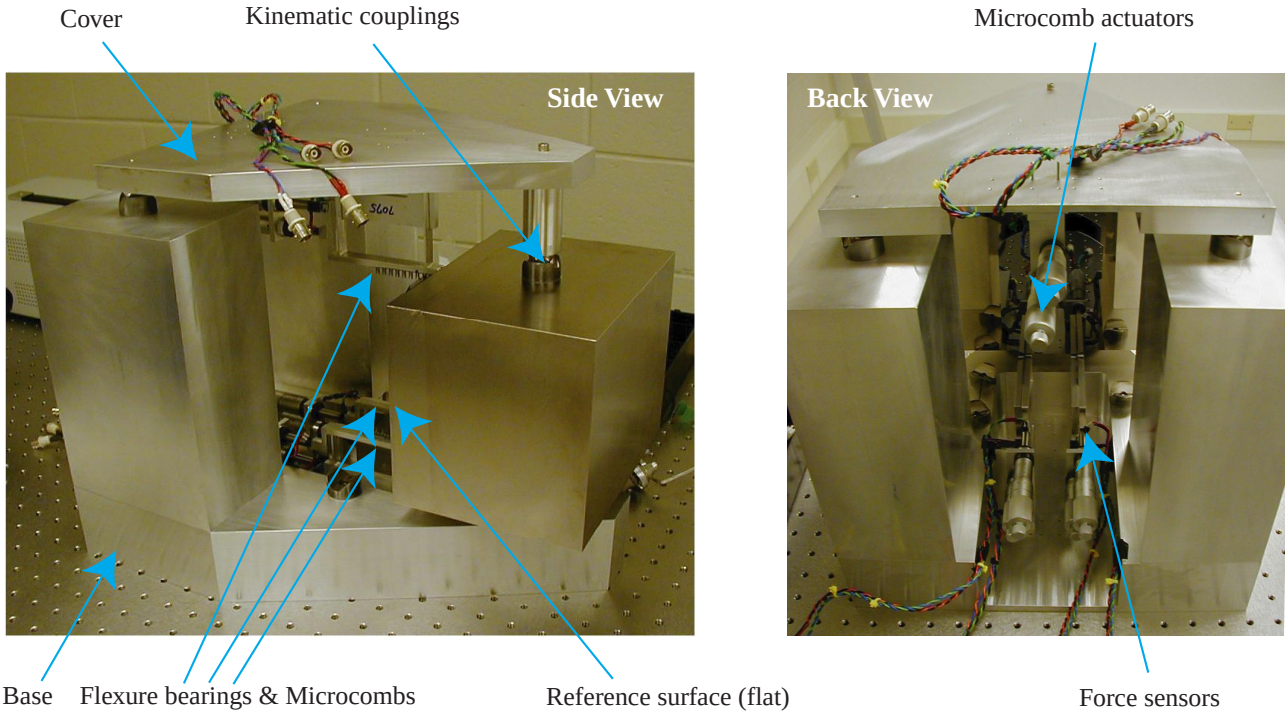


**Figure 4.** Foil assembly truss.

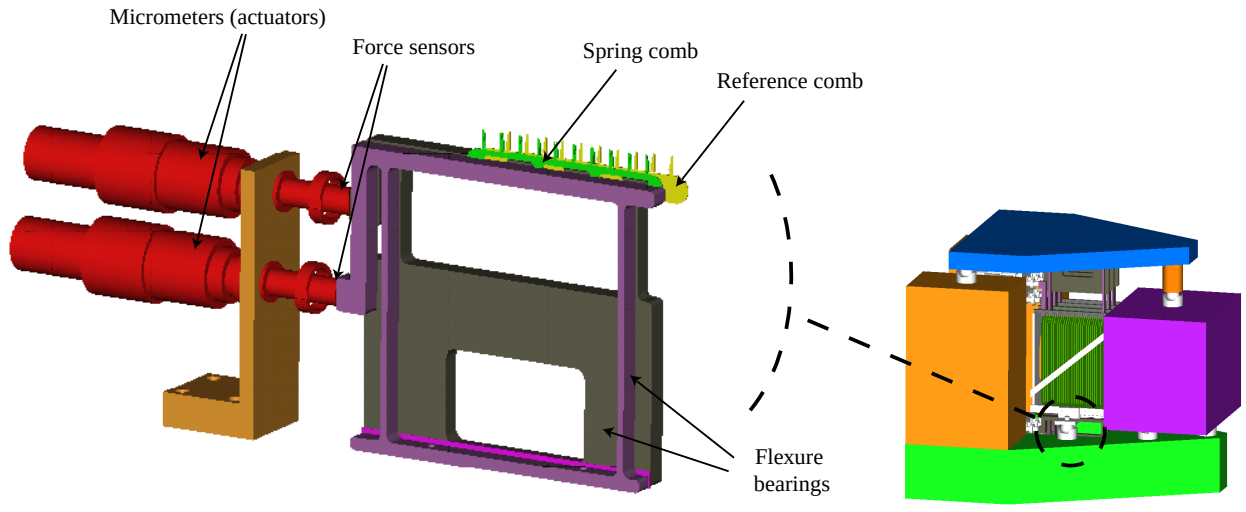


**Figure 5.** The flexure bearing assembly contains the microcombs, flexure bearings, force sensors, and micrometers.

have a resolution of 0.1 $\mu$m. This high resolution is critical to achieving the microcomb placement accuracy of 1 $\mu$m. Force sensors (Honeywell, sold by Cooper Instruments Model LPM 560, LPM 562) are placed in between the micrometers and the flexure bearings to detect when contact with the reference flat occurs, since then the stiffness of the system changes. Before contact, the force per unit displacement is a function of the stiffness of the flexure bearings, force sensors, micrometers, and micrometer holders. After contact, there is an additional stiffness component due to the Hertzian deformation of the microcomb. The force sensors are relatively insensitive to off-center plunger loading and have force ranges of 500 and 1500 grams-force for the reference and spring flexure bearings, respectively.

The structural parts of the assembly truss are stacked up with ball/v-block kinematic couplings at their interfaces. The ball and v-block design of these kinematic couplings theoretically allows repeatable assembly of the structure to less than 0.5 $\mu$m.[5] Fortunately, this error only impacts the foil assembly tolerances as a cosine term after flexure bearing actuation. The v-blocks are arranged such that the lines formed by the intersection of their respective faces intersect at the centroid of the triangle whose vertices are formed by the v-blocks themselves. This ensures uniform load distribution and prevents the faces from over-constraining the parts from misalignment.

The reference flat used as an alignment plane for the microcombs is a solid block of Aluminum 6061-T6 with 0.005 inches of electroless-plated nickel on its surface. The nickel is much harder than the aluminum to resist scratching during use. One face of the block is lapped and optically polished to 1 $\mu$m flatness P-V. Polished nickel was selected for a reference flat due to its low cost, hardness, and ease of machining.

A flight module containing the 0.4 mm thick optic foils was incorporated into the design of the assembly tool. Prior to assembly, thirty foils are loosely held in this module by a set of "coarse combs." The entire structure is then loaded into the precision assembly tool. The microcombs manipulate the foils into their aligned locations within oversized slots in these coarse combs. Glue is then injected into the coarse comb slots to secure the aligned foils in place. The flight module, containing the foils, is then removed and installed in the telescope. The flight module includes kinematic balls for the repeatable alignment with the base.

### 3.2. Experimental procedure and results

Numerous tests have been performed on the assembly truss to determine its ability to meet precision foil alignment goals of 1 $\mu$m. An autocollimator (Newport, model LAE500H) was used to measure the angular errors of a foil located in a "slot," which were then converted to displacements. Previous experiments performed on a static breadboard test assembly system have demonstrated a 1 $\sigma$ mounting slot repeatability error of about 0.11 $\mu$m in both axes.[6] This previous research defined repeatability as the standard deviation of a set of measurements collected by successively measuring, lifting, and replacing an optic foil against fixed reference microcomb teeth. This test was repeated with the new design and the data shows less than 0.05 $\mu$m for both pitch and yaw.

The current research involves a dynamic assembly truss, which strives to mimic the actual telescope foil alignment procedures. A static test was performed to obtain a baseline for repeatability. In this test, an optic foil was inserted into a slot, measured, then completely removed from the truss, reinserted, and remeasured. All mechanical parts on the truss were static. To test dynamic slot repeatability, two tests were performed. In the

**Table 1.** Assembly truss slot alignment repeatability results.

| single slot repeatability test | displacement error, one $\sigma$ ($\mu$m) | | | |
|---|---|---|---|---|
| | 0.4 mm thick silicon wafer | | 3 mm thick fused silica plate | |
| | pitch | yaw | pitch | yaw |
| fixed lid and combs | 0.26 | 0.39 | 0.59 | 0.23 |
| dynamic lid, fixed combs | 0.83 | 0.93 | 0.47 | 0.40 |
| dynamic lid and combs | 0.34 | 0.36 | 0.33 | 0.30 |

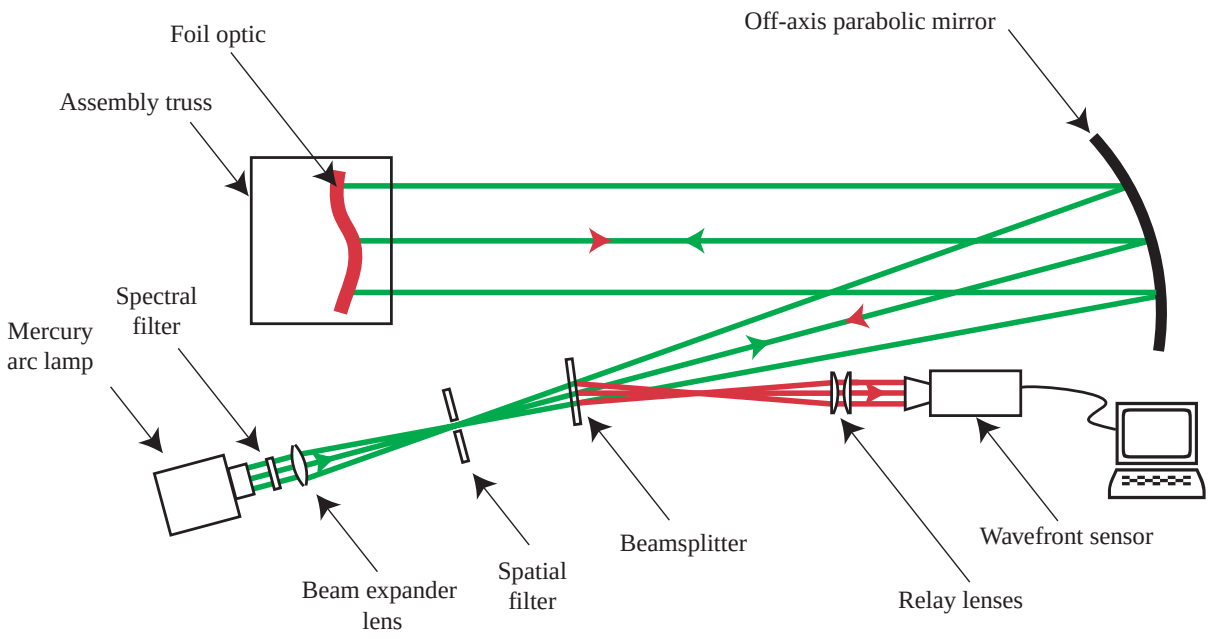


**Figure 6.** Shack-Hartmann metrology tool.

first test, the truss lid was removed and replaced as would be required for actual flight module assembly. The combs were not moved relative to the lid or base. The second dynamic test, which comes closest to actual flight module assembly, includes microcomb actuation to the planar reference flat in addition to lid reinstallation. These tests were conducted with both a 0.4 mm thick silicon wafer and a 3 mm thick fused silica plate coated with a reflective aluminum surface. Both materials were studied to understand the repercussions of thin foil deformation. Each test was performed approximately five times. Results from these tests are summarized in Tab. 1.

The results from the static test indicate that the repeatability of fully replacing an optic foil on the microcombs is approximately 0.35 $\mu$m in both axes. The second test includes the lid kinematic coupling repeatability error in addition. In this test, gravity deformation of the thin silicon wafer may account for the difference between the substrate results. The final test effectively cancels out the kinematic coupling error in the sensitive direction by actuating the combs to the reference flat. Hence, in the final test, the optic foil placement repeatability appears to dominate. Comparing the difference in the final test results for the different foil thicknesses, thin foil deformation does not appear to be a significant contributor to the overall error.

## 4. SHACK-HARTMANN SURFACE METROLOGY TOOL

Metrology is essential to successfully shaping and assembling foil optics. Concerning shaping, metrological feedback closes the loop on the manufacturing process. Quantifying figure errors permits the evaluation of process improvements. During assembly, micron level distortions to the foil optic may occur due to gravity or friction. Material thermal expansion mismatch may also cause low spatial frequency distortion. Study of these effects requires a metrology tool with a large viewing area, high angular resolution, and large angular range. Shack-Hartmann wavefront sensing technology was selected over phase shifting interferometry because it could meet these metrology requirements with lower costs, lower complexity, and vibration insensitivity.

### 4.1. Design

The optical design for the deep-UV Shack Hartmann metrology tool is shown in Fig. 6. The layout is similar to

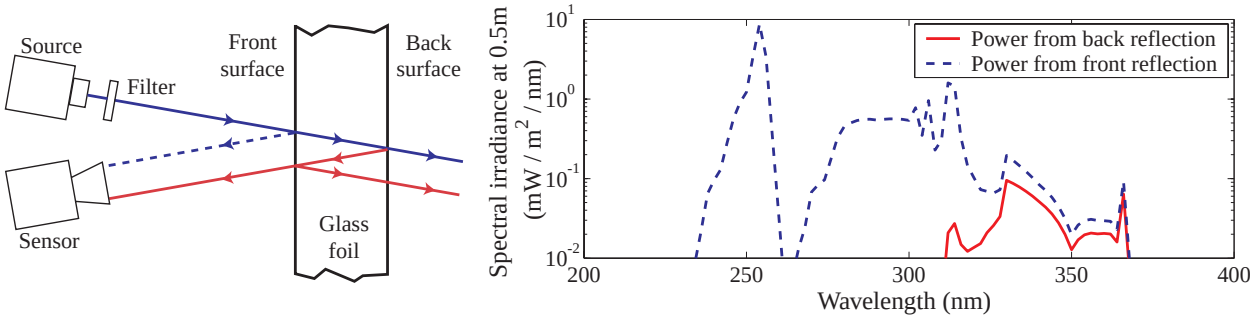


**Figure 7.** Irradiance reflected from the glass sheets into wavefront sensor as a function of wavelength.

a Keplerian telescope design, in that collimated input from the foil optic is demagnified to a collimated input to the wavefront sensor. This is accomplished using a large (200 mm diameter) off-axis parabolic mirror in conjunction with a relay lens. The magnification of the system and the advantage of this layout can be derived from the system matrix:

$$\begin{bmatrix} A & B \\ C & D \end{bmatrix} = \overbrace{\begin{bmatrix} 1 & 0 \\ L_2 & 1 \end{bmatrix}}^{\text{Propagation to } 2^{nd} \text{ lens from sensor}} \underbrace{\begin{bmatrix} 1 & -\frac{1}{f_2} \\ 0 & 1 \end{bmatrix}}_{\text{Refraction from } 2^{nd} \text{ lens}} \overbrace{\begin{bmatrix} 1 & 0 \\ f_1+f_2 & 1 \end{bmatrix}}^{\text{Propagation between lenses}} \underbrace{\begin{bmatrix} 1 & -\frac{1}{f_1} \\ 0 & 1 \end{bmatrix}}_{\text{Refraction from } 1^{st} \text{ lens}} \overbrace{\begin{bmatrix} 1 & 0 \\ L_1 & 1 \end{bmatrix}}^{\text{Propagation to } 1^{st} \text{ lens from foil}} = \begin{bmatrix} \frac{1}{M} & 0 \\ 0 & M \end{bmatrix} \quad (1)$$

where the $1^{st}$ lens is replaced by a parabolic mirror and the $2^{nd}$ is the relay lens. Choosing $L_1 = f_1 = 755.5$ mm and $L_2 = f_2 = 75.0$ mm, the system magnification M, given by matrix element D, reduces to $-\frac{f_2}{f_1} = 0.1$. The system has no effective optical power as indicated by the B element. Element C shows that the effective propagation distance is zero—the effects of diffraction are minimized at the image plane. The system matrix is diagonal, revealing that position and tilt are decoupled.

Deep-UV light is the most novel characteristic of the system. A 200 Watt broadband mercury arc lamp is spectrally filtered to allow mostly sub-visible wavelengths. Deep-UV light is exclusively required due to the optical transmission properties of the borosilicate glass foils (Schott, model D-263) proposed for the Constellation-X telescope optics. Light incident on the glass foil at wavelengths greater than 300 nm will partially transmit through the substrate and reflect off of its back surface. This will result in a doubled set of data on the wavefront sensor which will corrupt wavefront reconstruction. The non-ideal spectral filter on the arc lamp does permit some longer wavelength radiation to reflect off of the foil optic, as shown in Fig. 7. The theoretically computed irradiances take into consideration the spectral output of the arc lamp, the transmission curve of the spectral filter, and the optical properties of the glass to be tested. The ratio of the power into the camera from the front reflection to the back reflection, calculated from the respective areas under the curves, is approximately 34.3. This back reflection power is below the sensor noise floor, making the error signal negligible. For comparison, if a higher wavelength HeNe laser were used for illumination, the ratio of the power from the front to back reflection would be 1.3. This would make the wavefront reconstruction erroneous.

A Shack-Hartmann[7] wavefront sensor (Wavefront Sciences, model CLAS-2D SMD) is used to image the optic under test. A key feature of this instrument is a lenslet array which dissects the incoming wavefront into 64×64 segments. Each of these segments is focused onto a detector located at the lenslet focal plane. The engineering tradeoffs with the performance of this instrument have been studied by Greivenkamp *et al.*[8] By comparing the focal spot locations on the detector from a reference surface to those from an aberrant surface, a difference map is calculated. Spatially integrating the slopes of this map allows the wavefront shape to be reconstructed. The angular range of measurement involves the detector area allocated to each lenslet (area of interest or AOI). When the focal spot behind a lenslet appears near the edge of its AOI, crosstalk occurs and wavefront reconstruction is compromised, thereby limiting the angular range. The angular range for this

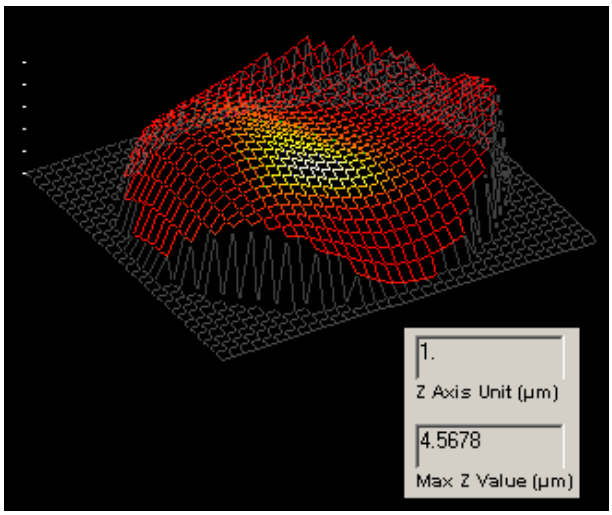


**Figure 8.** Reconstructed wavefront equivalent to a surface map at the object plane.

camera can be estimated from the lenslet diameter of 0.224 mm and operating focal length of 17.904 mm to be approximately ±6 mrad. The focal spot radius further reduces this range to ±5.1 mrad. The instrument's sensitivity hinges on its ability to accurately centroid the focal spots, a function of the pixel size, bit resolution, and focal length. For this instrument, the sensitivity can be calculated to be around ±1 $\mu$rad. Over a 10 mm lateral distance in the magnified object plane, these performance specifications correspond to a theoretically measurable P-V height of ±5 $\mu$m with a resolution of ±1 nm. Previous surface mapping of stock silicon wafers indicate spatial distortion of this frequency and magnitude, so this instrument will be able to track subsequent flatness improvements from the original stock material.

### 4.2. Experimental procedure and results

The surface metrology instrument has been successfully used to generate surface maps of large $\frac{\lambda}{30}$ reference flats, 0.45×100 mm diameter polished silicon wafers as commonly used in semiconductor industry, and 100×140×0.4 mm$^3$ glass sheets. A sample image is shown in Fig. 8. The repeatability of the measurements has been primarily limited by random variations in the arc lamp caused by arc migration on the electrodes and convection currents inside the lamp.[9] Averaging 100 successive images has mitigated the effects of these variations, reducing the range of P-V surface maps to 5.0 nm (0.5 nm root-mean-squared (RMS)) over a minimum 100 mm diameter object size while the setup is unchanged. To determine the repeatability of the instrument for a human-in-the-loop environment, specimens were measured, physically removed from the metrology station, replaced and remeasured. Both the reference surface and the silicon wafer specimens were studied; results were similar. Repeatability measurements ranged 35.6 nm P-V with a 13.2 nm standard deviation. RMS surface variations ranged 14.0 nm with a 5.1 nm standard deviation.

The accuracy of the system is difficult to quantify since aberrations in the lenses will contribute different angular errors to measurements at different spatial locations. To roughly estimate the overall accuracy of the system, two flats with factory-provided interferograms were measured. These interferograms reveal non-flatnesses of 2.6 nm RMS and 4.9 nm RMS, respectively. Comparing the two flats with the Shack-Hartmann system shows an average RMS surface difference of 17.6 nm. Overlapping the interferograms, the RMS deviation can be estimated to be $\sqrt{2.6^2 + 4.9^2} = 5.5$ nm. The difference between the Shack-Hartmann and interferometric data provides a crude estimation of the accuracy of the tool. Assuming root-sum-squared (RSS) stacking of errors, a conservative estimate of the accuracy yields $\sqrt{17.6^2 - 5.5^2} = 16.7$ nm RMS. Many factors contribute to the difference between the interferograms and Shack-Hartmann measurements. The mirrors are subjected to different temperatures and mounting forces between the instruments. Additionally, the uncertainty in the interferometric measurements is estimated to be $\frac{\lambda}{50} \approx 13$ nm P-V.

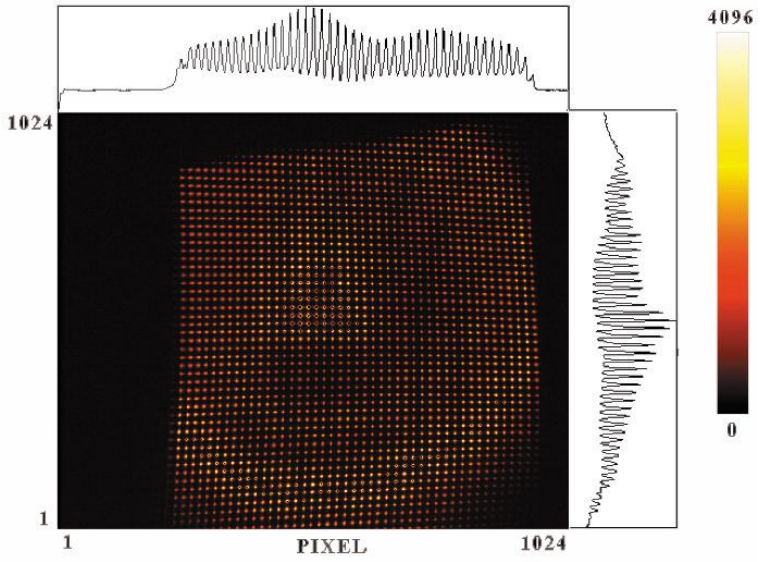


**Figure 9.** Raw data onto wavefront sensor from Schott D-263 glass sheet.

In operation, the user will make a reference image with a flat, then substitute the optic under test. Based on the above analysis, the test measurement will be accurate to ∼17 nm and repeatable to ∼5 nm, RMS.

Results from glass metrology show no indication of back reflections in the raw data. The array of focal spots is regular and the frequency of spots is as expected, one per AOI. Large warp in pre-figured stock glass sheets makes their entire surface unmeasurable. A sample of this raw data is shown in Fig. 9. Subset regions of the figure have been successfully measured to the accuracy and repeatability previously described.

## 5. CONCLUSIONS

Magneto-rheologic fluid polishing has been used to flatten stock silicon wafers to $<1\mu$m P-V. Reflection grating substrates will require flatness of this magnitude to meet the *Constellation–X* resolution goals. This manufacturing process can be further improved with more accurate surface metrology. This promising technique is under further study as a sole or complementary process for manufacturing the thin foil optics.

Using a precision assembly truss, slot repeatability has been studied in an environment which closely matches that of the actual telescope optics assembly. This work has demonstrated that the assembly technology can meet the 1 $\mu$m Constellation-X foil placement repeatability requirement. Future work will include study of the accuracy of the microcombs.

A Shack-Hartmann surface metrology tool has been developed that permits metrological feedback of optic foils under consideration for the Constellation-X mission. This feedback is crucial during the assembly procedure since gravity, friction, and other forces can distort the wafers beyond the assembly tolerance.

This instrument can be used to determine if a surface meets the current 500 nm global flatness manufacturing requirement. The surface mapping data is accurate to ∼17 nm and repeatable to ∼5 nm, RMS. Non-flat figures can also be studied up to a dynamic range of ± 250 $\mu$rad at the object plane. The 200 mm diameter viewing range can accommodate the proposed $140\times100$ mm$^2$ foil optic surface area.

Substantial progress has been made in foil optic shaping, metrology, and assembly. This technology will contribute to a successful *Constellation–X* telescope which will have a substantial increase in effective area, energy resolution, and energy bandpass over current missions.

## ACKNOWLEDGMENTS

We gratefully acknowledge the assistance of our colleagues at Columbia University and QED Technologies, Inc. The support of the students, staff, and facilities from the Space Nanotechnology Laboratory are also much appreciated. This work is supported by NASA Grants NAG5-5271 and NCC5-633.

## REFERENCES

1. C. G. Chen, R. K. Heilmann, P. T. Konkola, O. Mongrard, G. P. Monnelly, and M. L. Schattenburg, "Microcomb design and fabrication for high accuracy optical assembly," *J. Vac. Sci. Technol. B* **18**, pp. 3272–3276, 2000.
2. O. Mongrard, "High accuracy foil optics for x-ray astronomy," master's thesis, Massachusetts Institute of Technology, Department of Aeronautics and Astronautics, Sept. 2001.
3. R. Heilmann, G. Monnelly, O. Mongrard, N. Butler, C. Chen, L. Cohen, C. Cook, L. Goldman, P. Konkola, M. McGuirk, G. Ricker, and M. Schattenburg, "Novel methods for shaping thin-foil optics for x-ray astronomy," in *Proc. SPIE*, (4496), pp. 62–72, 2002.
4. Y. Muranaka, M. Inaba, T. Asano, and E. Furukawa, "Parasitic rotations in parallel spring movements," *Int. J. Japan Society of Precision Engineering* **25**, pp. 208–213, Sept. 1991.
5. M. L. Culpepper, A. H. Slocum, and F. Z. Shaikh, "Compliant kinematic couplings for use in manufacturing and assembly," in *International Mechanical Engineering Congress and Exposition*, (Anaheim, CA), Nov. 1998.
6. O. Mongrard, N. Butler, C. Chen, R. Heilmann, P. Konkola, M. McGuirk, G. Monnelly, G. Pati, G. Ricker, M. Schattenburg, and L. Cohen, "High precision assembly and metrology of x-ray foil optics," in *Proc. Sixteenth Annual ASPE*, (Crystal City, Virginia), Nov. 2001.
7. B. C. Platt and R. Shack, "History and principles of shack-hartmann wavefront sensing," *Journal of Refractive Surgery* **17**, pp. 573–577, 2001.
8. J. E. Greivenkamp, D. G. Smith, R. O. Gappinger, and G. A. Williby, "Optical testing using shack-hartmann wavefront sensors," in *Proc. SPIE*, (4416), pp. 260–263, (Boston), 2001.
9. Oriel Instruments, http://www.oriel.com, *The Book of Photon Tools*, 2001.